VII International Conference on Computational Methods in Marine Engineering
MARINE 2017
M. Visonneau, P. Queutey and D. Le Touzé (Eds)

ADJOINT-BASED OPTIMIZATION METHODS FOR FLOW PROBLEMS

Thorsten Grahs* **and Johann Turnow†**

* Institute of Scientific Computing
Technische Universität Braunschweig
Mühlenpfordtstrasse 23, 38106 Braunschweig, Germany
e-mail: t.grahs@tu-bs.de

† Chair of Modelling and Simulation
University of Rostock
Albert-Einstein-Str. 2, 8059 Rostock, Germany
email: johann.turnow@uni-rostock.de

Key words: Computational Methods, Optimization, Adjoint, Sensitivity Analysis

Abstract. Over the last decade, adjoint sensitivity analysis has become an established technique for the task of shape optimisation when many degrees of freedom are present. The success stems from the fact that the adjoint approach only needs one flow simulation for both the primal and the adjoint system, no matter how many design parameters are present. The derivation of the continuous adjoint approach is based on an augmented cost function which inheres the primal governing equations (here the RANS-equations) as constraints which have to be satisfied in the computational domain. Accordingly, the primal RANS equations are augmented with Lagrange multipliers and added to the thermal-fluid dynamic cost function. For shape optimisation, the variational formulation of the augmented cost function indicates the behaviour of the cost function with the variation of the shape, i.e. the variation of the surface mesh in normal direction.

We present the derivation and application of the continuous adjoint approach for the incompressible Reynolds-averaged Navier-Stokes (RANS) equations augmented with heat transfer. The derived approach is implemented into the framework of the C++ CFD toolbox OpenFOAM in order to derive a complete design cycle for shape optimisation. The derived optimisation process is applied to dimpled surface geometries in order to optimise cooling devices.

1 INTRODUCTION

Originally arising in control theory [1], adjoint sensitivity analysis has made its way into the area of fluid mechanics [2, 3]. Since then the method has become an established technique for shape and topology optimisation of fluid problems, especially when many degrees of freedom are present [4, 5]. The success stems from the fact that the adjoint approach only needs two flow simulations, one for the primal and one for the adjoint system, no matter how many design parameters are present. This is a clear advantage over standard parametric geometry

optimization, which needs usually as many flow solutions as parameter combinations are present. This benefit, especially for large application cases and consequently adjoint based optimization methods, has become an important tool in the optimization of industrially relevant application (e.g. [6–12]).

In this approach, we apply the the continuous adjoint approach to the incompressible Reynolds-averaged Navier-Stokes (RANS) equations augmented with heat transfer. We derive the according adjoint system and adjoint boundary conditions for maximizing heat flux over a certain boundary. The derived optimization process is applied to dimpled surface geometries (see [15,16]) in order to optimize cooling devices.

2 THE GENERAL OPTIMIZATION PROBLEM

Let I be a specific cost function defined on an admissible domain $\Omega \subset \mathbb{R}^N$ with boundary Γ. The domain Ω will be allowed to vary during the design process and is parametrized through a set of design variables $\boldsymbol{\beta}$. In addition, a set of given constraints $\boldsymbol{r}(\boldsymbol{s})$ has to be obeyed, typically a set of partial differential equations (governing equations) with state variables $\boldsymbol{s}$. We can formulate the problem by

$$\max_{\beta} I(\boldsymbol{s}, \boldsymbol{\beta}) \quad \text{subject to} \quad \boldsymbol{r}(\boldsymbol{s}, \boldsymbol{\beta}) = 0 \quad \text{in} \quad \Omega. \tag{1}$$

This means we adapt the domain Ω by changing the design parameter $\boldsymbol{\beta}$ in order to improve the cost function I.

The dependency of the cost function $I(\boldsymbol{s}, \boldsymbol{\beta})$ with respect to their parameters is expressed by their total variation:

$$\delta I \;=\; \delta_{\boldsymbol{s}} I + \delta_{\boldsymbol{\beta}} I \;=\; \underbrace{\frac{\partial I}{\partial \boldsymbol{s}} \delta \boldsymbol{s}}_{flow} + \underbrace{\frac{\partial I}{\partial \boldsymbol{\beta}} \delta \boldsymbol{\beta}}_{geometry} \;. \tag{2}$$

The necessary information for geometry variation comes from the so-called *sensitivity* $\partial I / \partial \boldsymbol{\beta}$ of the cost function with respect to the design parameters.The sensitivity reveals how the cost function is affected by an admissible variation $\delta \boldsymbol{\beta}$ of the design parameters $\boldsymbol{\beta}$. In our approach, we assume shape optimization, which means we want to deform the surface mesh of the simulation domain. Thus, the design parameters are the positions of the nodes of the surface mesh. Variation of the design parameter means in this context the variation in the direction of the corresponding normal vector, i.e. inward or outward movement of the surface node.

In general, the evaluation of the second right hand side term of (2) requires a solution of the flow field for each design parameter β_i [4, 5]. Thus, if one considers the variation of the surface nodes as design parameters, as we are going to do in the following, one has to carry out as many solution $\boldsymbol{r}(\boldsymbol{s}, \beta_i)$ as design parameters β_i are present. Typically, the number of surface nodes β_i is of the order $i = 10^6 - 10^7$. In order to avoid such computational effort, on changes from to the dual or adjoint formulation of the governing equations, what we demonstrate in the next sections.

3 THE PRIMAL EQUATION SYSTEM

The primal equation system of the optimization problem is constituted by the governing equations of the flow problem, i.e. the incompressible Navier-Stokes equations:

$$\begin{aligned} \partial_t(\rho\mathbf{u}) + (\mathbf{u}\cdot\nabla)\mathbf{u} &= -\nabla p + \nabla\cdot[2\nu\mathbf{D}(\mathbf{u})], \\ \partial_t\rho + \nabla\cdot\mathbf{u} &= 0. \end{aligned} \tag{3}$$

This equations forms the primal system with primal variables: pressure p and velocity $\mathbf{u} = (u_1,\ldots,u_3)^T$. Here, $\mathbf{D}(\mathbf{u}) = \frac{1}{2}[\nabla\mathbf{u} + (\nabla\mathbf{u})^T]$ is the stress tensor and ν the kinematic viscosity.

In order to treat heat transfer problems the system (3) is equipped with a thermal diffusion equation and thermal diffusivity α:

$$\frac{\partial T}{\partial t} + (\mathbf{u}\cdot\nabla)T = \nabla(\alpha\cdot\nabla T). \tag{4}$$

The primal flow field can be described by the state vector $\mathbf{s} = (\mathbf{u}, p, T)^T$, which is a solution of the system (3,4). Since we focus on steady state solutions, we omit the time-derivatives and rewrite the system in residual form:

$$\mathbf{r}(\mathbf{s}) = \begin{bmatrix} (r_1,r_2,r_3)^T \\ r_4 \\ r_5 \end{bmatrix} = \begin{bmatrix} (\mathbf{u}\cdot\nabla)\mathbf{u} + \nabla p - \nabla\cdot[2\nu\mathbf{D}(\mathbf{u})] \\ -\nabla\cdot\mathbf{u} \\ (\mathbf{u}\cdot\nabla)T - \nabla(\alpha\cdot\nabla T) \end{bmatrix} = \mathbf{0} \tag{5}$$

4 THE ADJOINT FORMULATION

In order to derive the adjoint system and the desired sensitivities we have to formulate an augmented cost function which obeys the governing equations as a constraint. This leads to a formulation of the adjoint system and adjoint boundary conditions. The necessary procedure will be demonstrated in the following.

4.1 The augmented cost function

The general approach of deriving the adjoint sensitivity analysis starts from an augmented objective function L, which is based of the cost function I augmented by the residual form of the state equation $\boldsymbol{r}(\boldsymbol{s},\boldsymbol{\beta}) = \mathbf{0}$, and the adjoint state variables $\hat{\boldsymbol{s}}$ acting as Lagrange multipliers. This approach is meaningful since the fulfilment of the governing equations acts as a constraint on the optimisation problem.

$$L(\boldsymbol{s},\boldsymbol{\beta}) = I(\boldsymbol{s},\boldsymbol{\beta}) + \int_\Omega \hat{\boldsymbol{s}}^T\boldsymbol{r}\,\mathrm{d}\Omega. \tag{6}$$

Since (6) depends on the solution of the continuous flow field $\boldsymbol{r}$ and the current design expressed by the vector of design variables $\boldsymbol{\beta}$ the total variation of L due to a change in Ω is

$$\delta L = \left(\frac{\partial I}{\partial \boldsymbol{s}} + \int_\Omega \hat{\boldsymbol{s}}^T\frac{\partial \boldsymbol{r}}{\partial \boldsymbol{s}}\,\mathrm{d}\Omega\right)\delta\boldsymbol{s} + \left(\frac{\partial I}{\partial \boldsymbol{\beta}} + \int_\Omega \hat{\boldsymbol{s}}^T\frac{\partial \boldsymbol{r}}{\partial \boldsymbol{\beta}}\,\mathrm{d}\Omega\right)\delta\boldsymbol{\beta}. \tag{7}$$

Choosing $\hat{\boldsymbol{s}}$ such that the first right hand side term in (7) vanishes identically, i.e. for all admissible states $\boldsymbol{s}$, we write:

$$\frac{\partial I}{\partial \boldsymbol{s}}\delta\boldsymbol{s} + \int\limits_{\Omega} \hat{\boldsymbol{s}}^T \frac{\partial \boldsymbol{r}}{\partial \boldsymbol{s}}\,\mathrm{d}\Omega\delta\boldsymbol{s}. \;=\; 0. \tag{8}$$

This choice of the adjoint state vector $\hat{\boldsymbol{s}}$ motivates the alternative viewpoint of the adjoint variables as Lagrangian multipliers [4]. Consequently, the sensitivity of (6) reduces to

$$\delta_\beta L \;=\; \underbrace{\frac{\partial I}{\partial \boldsymbol{\beta}}\delta\boldsymbol{\beta}}_{=\delta_{\boldsymbol{\beta}} I} + \int\limits_{\Omega} \hat{\boldsymbol{s}}^T \underbrace{\frac{\partial \boldsymbol{r}}{\partial \boldsymbol{\beta}}\delta\boldsymbol{\beta}}_{=\delta_{\boldsymbol{\beta}}\boldsymbol{r}}\,\mathrm{d}\Omega. \tag{9}$$

4.2 Sensitivity of the cost function

The sensitivity of the cost function with respect to the design parameters (9) can be reformulated in order to shift the variation of the state vector from $\boldsymbol{\beta}$ to $\boldsymbol{s}$. By using the fact that the variation of $\boldsymbol{r}$ vanishes for any admissible variation of $\boldsymbol{s}$, we deduce

$$0 = \delta\boldsymbol{r} \;=\; \delta_{\boldsymbol{\beta}}\boldsymbol{r} + \delta_{\boldsymbol{s}}\boldsymbol{r}, \tag{10}$$

and thus

$$\delta_{\boldsymbol{\beta}}\boldsymbol{r} = -\delta_{\boldsymbol{s}}\boldsymbol{r}. \tag{11}$$

Substituting (11) into (9) yields

$$\delta_\beta L \;=\; \delta_{\boldsymbol{\beta}} I \;-\; \int\limits_{\Omega} \hat{\boldsymbol{s}}^T \delta_{\boldsymbol{s}}\boldsymbol{r}\,\mathrm{d}\Omega. \tag{12}$$

Now we are able to calculate (9) by the variation due to the design parameters and an inner product between the variation of the governing equation with respect to the design variables $\boldsymbol{\beta}$ and the adjoint state vector $\hat{\boldsymbol{s}}$. The latter is just the solution of the adjoint system, i.e. the solution of our adjoint flow equation.

4.3 The adjoint equation system

Starting point of the adjoint approach is variation of the Lagrange function (8). This variation has to be identically zero, i.e.

$$\delta_{\boldsymbol{s}} L = \delta_{\boldsymbol{s}} I + \int_{\Omega} \hat{\boldsymbol{s}}^T\, \delta_{\boldsymbol{s}}\boldsymbol{r}\,\mathrm{d}\Omega \;\equiv\; 0. \tag{13}$$

The vector $\hat{\boldsymbol{s}}$ can be interpreted from two different viewpoints: as vector of the Lagrange multipliers, or as adjoint state vector with adjoint velocity, adjoint pressure and adjoint temperature, i.e. $\hat{\boldsymbol{s}} = (\hat{\boldsymbol{u}}, \hat{p}, \hat{T})^T$.

After several transformations and the demand that the derived equations have to be fulfilled for all variations of the primal state one derives the corresponding inhomogeneous continuous adjoint system (see [13] for details):

$$\begin{aligned} \mathbf{D}(\hat{\boldsymbol{u}})\boldsymbol{u} + \nabla\cdot(2\nu\mathbf{D}(\hat{\boldsymbol{u}})) - \nabla\hat{p} + T\nabla\hat{T} &= \frac{\partial I_\Omega}{\partial \boldsymbol{u}}, \\ \nabla\cdot\hat{\boldsymbol{u}} &= \frac{\partial I_\Omega}{\partial p}, \\ \boldsymbol{u}\cdot\nabla\hat{T} + \nabla\cdot(\alpha\nabla\hat{T}) &= \frac{\partial I_\Omega}{\partial T}. \end{aligned} \tag{14}$$

In the case one assumes only surface contributions, i.e. one focusses on shape rather than volume or topology optimisation, one has to deal with the homogeneous adjoint system:

$$\begin{aligned} \mathbf{D}(\hat{\boldsymbol{u}})\boldsymbol{u} + \nabla\cdot(2\nu\mathbf{D}(\hat{\boldsymbol{u}})) - \nabla\hat{p} + T\nabla\hat{T} &= \mathbf{0}, \\ \nabla\cdot\hat{\boldsymbol{u}} &= 0, \\ \boldsymbol{u}\cdot\nabla\hat{T} + \nabla\cdot(\alpha\nabla\hat{T}) &= 0. \end{aligned} \tag{15}$$

4.4 Adjoint boundary conditions

In order to close the system (15) we have to fulfil appropriate boundary conditions.

Here one distincts between conditions which have to be fulfilled at the different types of boundaries, i.e. inlet, wall and outlet, in order to incorporate the different situation at each boundary type (see [7]).

To this use we split the adjoint velocity vector into tangential and normal parts, i.e.

$$\hat{\boldsymbol{u}} \;= \hat{\boldsymbol{u}}_t + \hat{\boldsymbol{u}}_n \;=\; u_t\boldsymbol{t} + u_n\boldsymbol{n} \quad \text{with} \quad \boldsymbol{t}\perp\boldsymbol{n}. \tag{16}$$

With these assumptions and appropriate primal boundary conditions, we derive boundary conditions for the adjoint variables at the inlet, wall and outlet:

Inlet

$$\hat{\boldsymbol{u}}_t \;=\; \mathbf{0}, \quad \hat{u}_n \;=\; -\frac{\partial I_\Gamma}{\partial p}, \quad \frac{\partial\hat{p}}{\partial\boldsymbol{n}} \;=\; 0, \quad \hat{T} = 0. \tag{17}$$

At the inlet, we assume Dirichlet conditions for primal velocity and primal temperature, and Neumann conditions for the primal pressure.

Wall

$$\hat{\boldsymbol{u}}_t \;=\; \mathbf{0}, \quad \hat{u}_n \;=\; -\frac{\partial I_\Gamma}{\partial p}, \quad \frac{\partial\hat{p}}{\partial\boldsymbol{n}} \;=\; 0, \quad \frac{\partial\hat{T}}{\partial\boldsymbol{n}} \;=\; -\frac{1}{\alpha}\frac{I_\Gamma}{\partial T}. \tag{18}$$

At walls, we assume no-slip conditions for the primal velocity, Dirichlet conditions for the primal temperature, and Neumann conditions for the primal pressure.

Outlet

$$\begin{aligned} u_n\hat{\boldsymbol{u}}_t + \nu(\boldsymbol{n}\cdot\nabla)\hat{\boldsymbol{u}}_t &= \frac{\partial I_\Gamma}{\partial \boldsymbol{u}_t}, \\ \hat{\boldsymbol{u}}\cdot\boldsymbol{u} + \hat{u}_n u_n + \nu(\boldsymbol{n}\cdot\nabla)\hat{u}_n + T\hat{T} + \frac{\partial I_\Gamma}{\partial \boldsymbol{u}_n} &= \hat{p} \\ u_n\hat{T} + \alpha\frac{\partial\hat{T}}{\partial\boldsymbol{n}} &= \frac{\partial I_\Gamma}{\partial T} \end{aligned} \tag{19}$$

The boundary conditions are generally in the form that they contain surface contribution I_Γ. Choosing a concrete cost function leads to specific adjoint boundary conditions.

5 OPTIMIZATION PROCEDURE

Obviously the optimization process depends on the overall design goal, i.e. minimizing or maximising the cost function. The link between optimization of the cost function and parameter variation is the total variation of the augmented cost function (6), i.e. the sum of the total variation with respect to the state vector $\boldsymbol{s}$ and the design parameters $\boldsymbol{\beta}$:

$$\delta L \quad = \delta_{\boldsymbol{s}} L + \delta_{\boldsymbol{\beta}} L. \tag{20}$$

The variation with respect to the state vector $\boldsymbol{s}$ directly leads to the solution of the adjoint system and was demonstrated in the foregoing section. What remains is the variation of the Lagrangian L with respect to the normal displacement of the boundary, which was

$$\delta_{\boldsymbol{\beta}} L = \delta_{\boldsymbol{\beta}} I + \delta_{\boldsymbol{\beta}} \int_{\Omega} \boldsymbol{s}^T \boldsymbol{r}\, \Omega. \tag{21}$$

These are the sensitivities of the system with respect to the design parameter $\boldsymbol{\beta}$. They keep the essential information how to deform the geometry in order to improve the cost function.

5.1 Sensitivities

In order to derive the sensitivity information one has to evaluate the variation of the state vector $\boldsymbol{s}$ with respect to the surface variation. Following the approach in [5] we linearised around a surface node $\boldsymbol{x}_n$ with $\boldsymbol{s}(\boldsymbol{x}_n + \beta_i) = \boldsymbol{s}(_n) + \partial\beta_i + O(\beta_i^2)$ and approximate the variation as

$$\delta_\beta \boldsymbol{s} \;=\; \delta_\beta \boldsymbol{s} \cdot \delta\beta \;\approx\; \partial_{\boldsymbol{n}} \boldsymbol{s} \cdot \delta\beta \tag{22}$$

This yields locally

$$\delta_\beta L \;=\; \delta_\beta I + \;\partial_{\boldsymbol{n}} \boldsymbol{s} \cdot \partial_{\boldsymbol{s}} I_\Gamma \tag{23}$$

Following the derivation in [7], i.e. considering no-slip condition at walls and the adjoint boundary conditions, the local surface sensitivity of a normal displacement of the surface is

$$\frac{\partial L}{\partial \beta_i} \approx -\nu \frac{\partial \boldsymbol{u}_t}{\partial \boldsymbol{n}_i} \frac{\partial \hat{\boldsymbol{u}}_t}{\partial \boldsymbol{n}_i} - \alpha \frac{\partial T}{\partial \boldsymbol{n}_i} \frac{\partial \hat{T}}{\partial \boldsymbol{n}_i} \;=:\; \sigma_i \tag{24}$$

with sensitivity vector $\boldsymbol{\sigma} = (\sigma_1, \ldots, \sigma_N)^T$, corresponding surface normal vector $\boldsymbol{n}_i$ and N the number of surface nodes.

5.2 Mesh deformation

The sensitivities represent the information how to deform the geometry, especially in which direction: inward or outward movement of the surface node. In general, the resulting sensitivity vector field will be highly distorted. In order to derive a smooth deformation vector field and thus a continuous geometry update one has to smooth the sensitivity field $\boldsymbol{\sigma}$. This is usually carried out by solving a Laplace equation for $\boldsymbol{\sigma}$ with a suitable diffusivity γ:

$$\nabla \cdot (\gamma \nabla \boldsymbol{\sigma}) \quad = 0 \tag{25}$$

which results in a smoothed sensitivity field $\tilde{\boldsymbol{\sigma}}$, which is used to perform the mesh update. The mesh update is carried out with a standard mesh motion approach in OpenFOAM.

5.3 The general design cycle

The overall goal of the design process is to derive a method of a successive improvement of the cost function based of the derived sensitivity information from the solution of the primal and the adjoint system. This procedure is an iterative process, meaning we have to apply the adjoint-based sensitivity analysis to the updated geometry in a repeated manner until it is converged or a prescribed design goal is reached. The resulting design loop can be formulated via the following steps:

For i:=1,N

- *Step 1:* *Solve primal equation system* (5).
- *Step 2:* *Solve the adjoint equation system* (15).
- *Step 3:* *Compute the sensitivity information* (24).
- *Step 4:* *Update the geometry based on Step 3.*
- *Step 5:* *Evaluate the cost function* I_i.
- *Step 6:* *Proceed if* $|I_i - I_{i-1}| > \varepsilon$

The ingredients of this optimization cycle, i.e. primal and adjoint solver, sensitivity computation, cost function evaluation and mesh deformation, are implemented in and use tools from the open-source CFD toolbox OpenFOAM [14].

6 APPLICATION

As a proof-of-concept we apply the approach to a concave dimpled plate [15]. Compared to ribs and fins, dimpled geometries show the best thermal-hydraulic performance defined as the ratio between the heat exchange and the pressure loss (see [16] for details). Our design goal is to maximise the wall heat flux on the lower boundary with the dimple.

6.1 The domain

We start from a rectangular domain with length $x = 0.276\,\mathrm{m}$, width $y = 0.08\,\mathrm{m}$, and height $z = 0.03\,\mathrm{m}$. The lower and upper faces are wall boundaries, the lateral ones are handled as cyclic boundaries. The lower boundary is equipped with a dimple with diameter $\mathrm{d} = 0.048\,\mathrm{m}$. and height $\mathrm{h} = 0.012\,\mathrm{m}$. The overall simulation domain and the lower wall with dimple are represented in Figure 1.

Initial conditions for the simulations at the inlet are: velocity $U = 5$ m/s and temperature $T = 330$ K. At wall boundaries we have: velocity $U = 0$ m/s and temperature $T = 293$ K.

6.2 Cost function

The design goal is to maximise the heat flux at the lower boundary. Consequently, the cost function is chosen as the integral of the heat flux through the bottom face i.e. the normal derivation of the temperature field on this patch:

$$I = \int_{wall} \frac{\partial T}{\partial \boldsymbol{n}} \mathrm{d}\Gamma \tag{26}$$

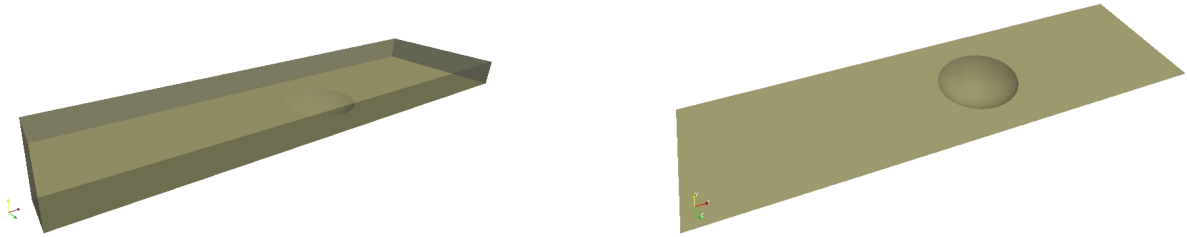

Figure 1: Simulation domain (left) and lower wall with dimple (right)

6.3 Results

In the following we present and discuss the results of the application of the optimization cycle from section 5.3 to the above described geometry in order to improve the cost function (26).

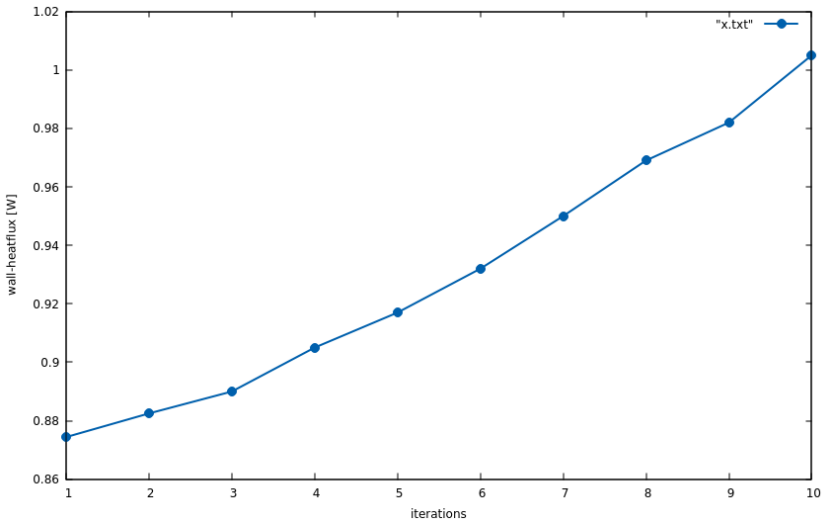

Figure 2: Wall heat flux vs. design iteration

Figure 2 represents the improvement of the wall heat flux on the lower boundary due to the design cycles iterations. It is worth to note that the pressure loss of the optimized geometry is merely increased by approx. 3%, while the wall heat flux is improved by approx. 15%.

A comparison between the shape of the initial dimple geometry and the optimized one is depicted in Figure 3. It can be clearly seen that the algorithm flattens the upstream edge of the dimple geometry while the downstream edge is slightly raised.

Flow fields for velocity and temperature of simulations of the initial and the optimized dimple geometry are depicted in Figure 4 and Figure 5, respectively. One clearly sees how velocity and temperature propagate into the dimpled domain, which results in an improved heat-flux at the lower boundary.

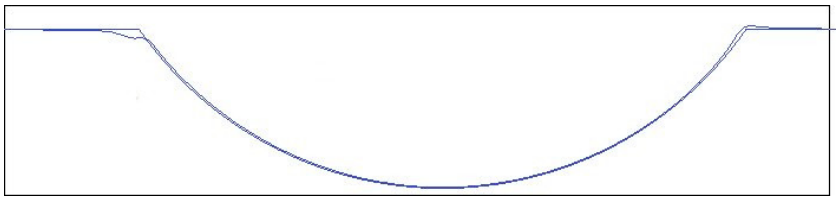

Figure 3: Comparison of initial and optimized dimple shape (longitudinal cut)

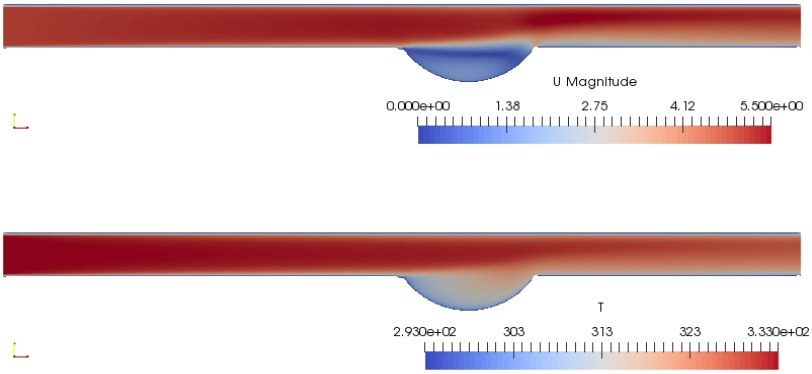

Figure 4: Velocity (top) and temperature (bottom) of the initial geometry

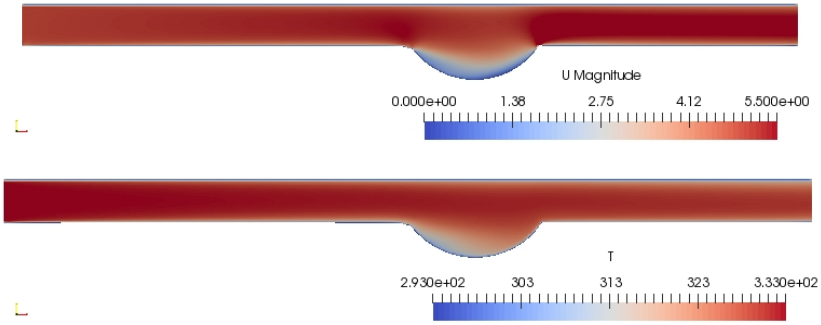

Figure 5: Velocity (top) and temperature (bottom) of the optimized geometry

7 SUMMARY AND OUTLOOK

We derived a continuous adjoint formulation of the steady-state, incompressible Navier-Stokes equations augmented with a diffusion equation for the temperature. The derived general adjoint system was adapted to specific maximisation of the heat flux at walls. The adjoint solver and adjoint boundary conditions were implemented into the CFD toolbox OpenFOAM in order to derive an optimization process involving mesh deformation based on the adjoint sensitivity

analysis derived from the primal and the adjoint solution of the system.

As a proof-of-concept this optimization approach was applied to a dimpled channel geometry. The results presented here a quite promising, since we were able to increase the wall heat flux on the lower boundary by approx. 15% while the pressure drop just increase slightly by approx. 3%. Nevertheless, further improvement and validation of the approach is necessary.

Future work will focus on the mesh deformation algorithm, e.g. with a radial-basis function approach, as well as the incorporation of additional cost function and a combination of these cost functions. Especially the combination of maximising heat-transfer and minimising pressure loss will be the next research topic in order to further improve heat exchangers for ducted flows.

REFERENCES

[1] Lions, J. L., *Optimal Control of Systems Governed by Partial Differential Equations*. Springer 1971.

[2] Pironneau, O., On optimum design in fluid dynamics. *J. Fluid. Mech.*, **64**, 97–110, (1974).

[3] Jameson, A., Aerodynamic Design via control theory. *J. Sci. Comput.*, **3**, 233–260, (1988).

[4] Giles, M. B., Pierce, N. A., An introduction to the adjoint approach to design. *Flow, Turbulence and Combustion*, **65** (3), 393–415, (2000).

[5] Soto, O., Löhner, R., On the computation of flow sensitivities from boundary integrals, *AIAA-04-0112*, (2004).

[6] Othmer, C., Grahs, T., Approaches to fluid dynamic optimization in the car development process, *EUROGEN 2005*, Munich (2005).

[7] Othmer, C., A continuous adjoint formulation for the computation of topological and surface sensitivities of ducted flows. *Int. J. Num. Meth. Fluids*, **58**, 861–877, (2008).

[8] Stück, A., Rung, T., Adjoint RANS for Hull-Form Optimisation, *12th Numerical Towing Tank Symposium*, Cortona, Italy (2009).

[9] Hinterberger, C., Olesen, M., Industrial application of continuous adjoint flow solvers for the optimization of automotive exhaust systems. *Proc. ECCOMAS Thematic Conf CFD & Optimization*, Antalya, Turkey, ECCOMAS (2011).

[10] Lincke A, Rung T., Adjoint-based sensitivity analysis for Buoyancy-driven incompressible Navier-Stokes equations with heat transfer. *Proc. 8th Int. Conf. on Eng. Comp. Tech.*, Dubrovnik, Croatia (2012).

[11] Funke, S. W., Farrell, P. E., Piggotta, M. D., Tidal turbine array optimisation using the adjoint approach, *Renewable Energy*, **63**, 658673, (2014).

[12] Othmer, C., Adjoint methods for car aerodynamics. *Mathematics in Industry*, **4** (6), 861–877, (2014).

[13] Grahs, T., Turnow, J., Derivation of a continuous adjoint formulation for the shape optimization of flows with heat transfer, *Informatik-Bericht, TU Braunschweig*, to appear, (2017).

[14] Weller, H. G., Tabor, G., Jasak, H., Fureby, C., A Tensiorial Approach To Computational Continuum Mechanics using Object Oriented Techniques, *Computers in Physics*, **12** (6), 620–631, (1998).

[15] Turnow, J., Zhdanov, V., Kornev, N., Hassel, E., Flow structures and heat transfer on dimples in a staggered arrangement, *Heat and Fluid Flow*, **35**,168–175, (2011).

[16] Ligrani, P. M., Oliveira, M. M., Blaskovich T., Comparison of heat transfer augmentation techniques *AIAA Journal*, **41** (3), 337–361, (2003).